JOURNAL OF MATERIALS SCIENCE 26 (1991) 3457–3462

Effect of high-temperature deformation on the texture of a two-phase titanium alloy

A. W. BOWEN, D. S. McDARMAID, P. G. PARTRIDGE
Materials and Structures Department, Royal Aerospace Establishment, Farnborough, GU14 6TD, UK

Changes in the texture of both the α- and β-phases of the two-phase alloy Ti–6Al–4V have been determined in order to clarify the mechanisms of high-temperature deformation. A strain of ~1.5 was applied to the alloy at 928 °C, at strain rates representative of superplastic and non-superplastic conditions. The α-phase texture changed very little with strain rate whereas that for the β-phase was much more sensitive. The β-phase texture was weakened at superplastic strain rates but developed a fibre texture at non-superplastic rates. It is postulated that under superplastic conditions the alloy deforms predominantly by grain boundary sliding of the soft β-phase grains, with the hard primary α-phase grains remaining in their original orientations and the measured loss in texture intensity being attributed to the loss in texture of the secondary α-phase only. Under non-superplastic conditions there is a greater contribution from plastic deformation in the β-phase which, in turn, can enhance the secondary α-phase texture.

1. Introduction

In the study of superplasticity in two-phase alloys an assessment of the extent of deformation in the individual phases is an important part of the overall microstructural evaluation (see, for example, the results reviewed by Kashyap *et al.* [1]). Analysing textures before and after deformation can form part of this assessment, and where this has been carried out for both phases [2–4] it has been shown that each phase can behave quite differently, with textures being retained more in one phase than the other. However, the relationship between these changes and superplastic deformation can only be established when there are no phase transformations during cooling to room temperature, since these would produce a microstructure different from that at the superplastic deformation temperature.

A good example of a two-phase alloy in which the above effect occurs is Ti–6Al–4V, for which some texture data have already been reported [5–9]. This paper describes the results of further texture analyses that help to clarify the relationship between texture and superplastic deformation in the α- and β-phases of this alloy, pointing out some of the factors to be aware of when studying alloys that undergo phase transformations when cooled to room temperature.

2. Experimental procedure

The alloy studied was a hot-rolled rectangular section (160 mm × 35 mm) bar of Ti–6Al–4V. Its composition (wt %) was: 6.34Al; 4.35V; 0.18Fe; < 0.006H; < 0.1N; > 0.150; balance Ti. Uniaxial tests were carried out using round bar test pieces cut from the longitudinal (L), transverse (T) and short transverse (ST) directions. Fuller details are given elsewhere [5, 6]. Test conditions representative of superplastic and non-superplastic strain rates at 928 °C were chosen, namely 4.2×10^{-4} and $1.05 \times 10^{-2}\,s^{-1}$, respectively, and texture and diffractometer analyses were carried out on cross-sections (normal to the tensile axis) of test pieces from all three directions after deforming to strains up to ~ 1.5 (Table I).

$(1\,0\,\bar{1}\,0)$, (0 0 0 2) and $(1\,0\,\bar{1}\,1)$ pole figures were measured for the α-phase, although only those for (0 0 0 2) will be presented here since they are representative of changes in all three types of pole figure. The pole figures measured for the β-phase were (1 1 0) and (2 0 0). The intensities in all pole figures were plotted relative to those from a random cold-pressed and sintered sample of Ti–6Al–4V. The initial texture analyses were carried out on a Philips texture goniometer and the more recent analyses on a Siemens texture goniometer. In both cases CuK_α radiation was used.

Particular care had to be exercised in the measurement of the β-phase pole figures because

(a) the (1 1 0) β-phase reflection is between the (0 0 0 2) and $(1\,0\,\bar{1}\,1)$ α-phase reflections, and

(b) there is only ~ 10% β-phase present at room temperature (although the phase proportions are 50:50 at 928 °C [7]).

Careful goniometer alignment was therefore necessary, as well as the use of narrow divergence and receiving slits, to measure the (1 1 0) pole figures. An important consequence of using a narrow receiving slit was a more marked defocusing effect, with the result that meaningful data in the (1 1 0) pole figures are limited to 50° tilt as opposed to the more conventional 75° tilt. A factor that mitigated this limitation

0022–2461/91 $03.00 + .12

TABLE I Deformation conditions studied

Direction	Strain rate (s^{-1})	Strain[a]
L	4.2×10^{-4}	1.33
	1.05×10^{-2}	1.51
T	4.2×10^{-4}	1.48
	1.05×10^{-2}	1.42
S	4.2×10^{-4}	1.27
	1.05×10^{-2}	1.38

[a] Strain = $\ln(A_0/A_f)$ where A_0 and A_f are the original and final cross-sectional areas, respectively. Test pieces were slowly cooled from 928 °C [5–7].

was the well-resolved narrow peaks for both phases (indicative of low residual internal strains [10, 11]), which meant that there were no gross losses in integrated peak intensities because of the use of the narrow receiving slit. (This is a factor to consider in all pole figure measurements when there are large differences in peak widths [12].)

Confirmatory evidence on the correctness of the (1 1 0) pole figures could not be obtained from the (2 2 0) reflection because of very low intensities. However, the (2 0 0) reflection, which is free from interference from nearby α-phase reflections, could be measured up to tilt angles of 75°. All specimens were also analysed in a Philips diffractometer, using CuK_α radiation, to establish the profiles of the (1 0 $\bar{1}$ 0), (0 0 0 2), (1 0 $\bar{1}$ 1) and (1 1 0) reflections.

3. Results

3.1. As-received condition

The starting texture of the alloy was characterized by a strong basal-edge texture in the α-phase [13] (Fig. 1a) and by its corresponding texture in the β-phase (Fig. 1d) (i.e. related to the α-phase through the Burgers relationship [14] with (0 0 0 2) ∥ (1 1 0)). Note, however, that there is a high degree of variant selection [13] which favours the (1 1 0) planes parallel to the edge of the bar.

The (0 0 0 2) and (1 1 0) pole figures for the as-received condition are shown as the starting point in the results given below for each of the three directions, with the stress axis at the centre of each pole figure of the strained test pieces.

3.2. L-orientation test pieces

The change in α-phase texture for the superplastically deformed test pieces (i.e. after a strain rate of $4.2 \times 10^{-4} s^{-1}$) is shown in Fig. 1b. There was no change in pole positions but there was a decrease in intensity from 7R (R = random) to 3R. The corresponding change in the β-phase is shown in Fig. 1e. In contrast to the α-phase changes, there was a large change in both peak positions and intensities such that the texture was very much weakened.

After non-superplastic deformation at $1.05 \times 10^{-2} s^{-1}$ there was a smaller reduction in α-phase texture intensity (Fig. 1c) than at the superplastic deformation rate. The corresponding β-phase texture, however, was totally different, with evidence for the development of a ⟨1 1 0⟩ fibre texture (Fig. 1f).

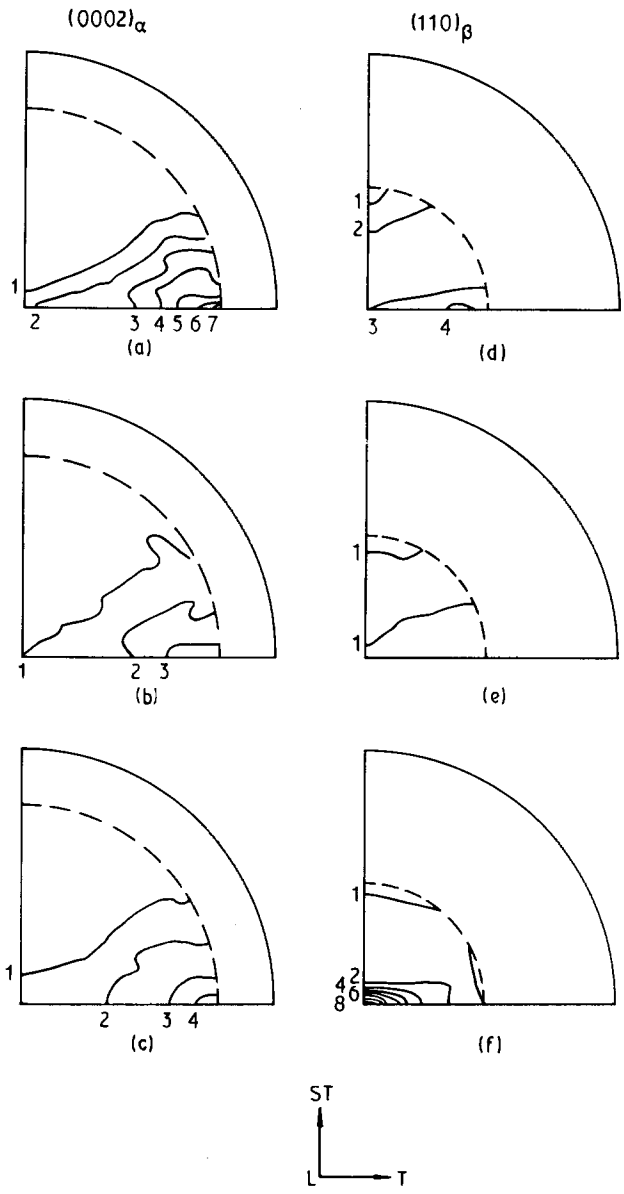

Figure 1 (0 0 0 2)$_\alpha$ and (1 1 0)$_\beta$ pole figures for longitudinally stressed test pieces of Ti–6Al–4V: (a, d) as-received; (b, e) after superplastic deformation at $4.2 \times 10^{-4} s^{-1}$; (c, f) after non-superplastic deformation at $1.05 \times 10^{-2} s^{-1}$ (contours × random).

The marked sensitivity to strain rate of the β-phase was also apparent in the (2 0 0) pole figures (Fig. 2). Note that they show the same trends as the (1 1 0) pole figures (Fig. 1d to f) and thus confirm that there was no inclusion of either the (0 0 0 2) or (1 0 $\bar{1}$ 1) α-phase reflections in the (1 1 0) pole figures. In the as-received condition the (2 0 0) pole figure showed strong poles at ~30° to the longitudinal direction and inclined towards the ST direction with isolated small peaks elsewhere (Fig. 2a). The strong 30° peaks disappeared after superplastic deformation and there were many more small isolated peaks (Fig. 2b). After non-superplastic deformation (Fig. 2c) the pole figure still showed some similarity to that for the as-received condition (Fig. 2a).

Diffractometer traces for the two conditions were consistent with the information at the centre of each pole figure (where the geometries were essentially the same), namely an increase in the intensity of (0 0 0 2) relative to (1 0 $\bar{1}$ 0) and (1 0 $\bar{1}$ 1) and a decrease in intensity of (1 1 0) relative to (0 0 0 2) under superplastic

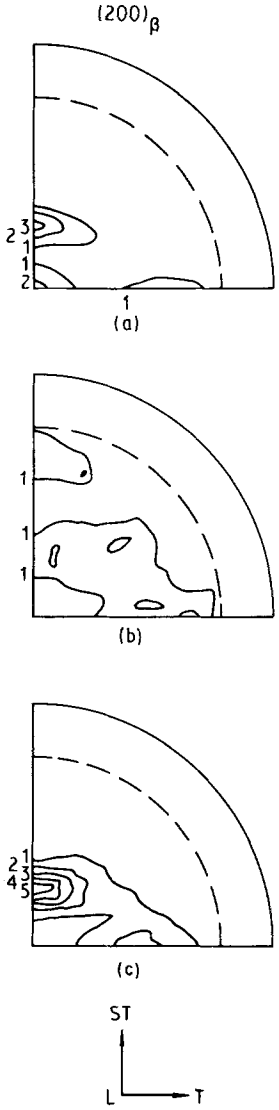

Figure 2 $(2\,0\,0)_\beta$ pole figures for longitudinally stressed test pieces of Ti–6Al–4V: (a) as-received, (b) after superplastic deformation at $4.2 \times 10^{-4} s^{-1}$, (c) after non-superplastic deformation at $1.05 \times 10^{-2} s^{-1}$ (contours × random).

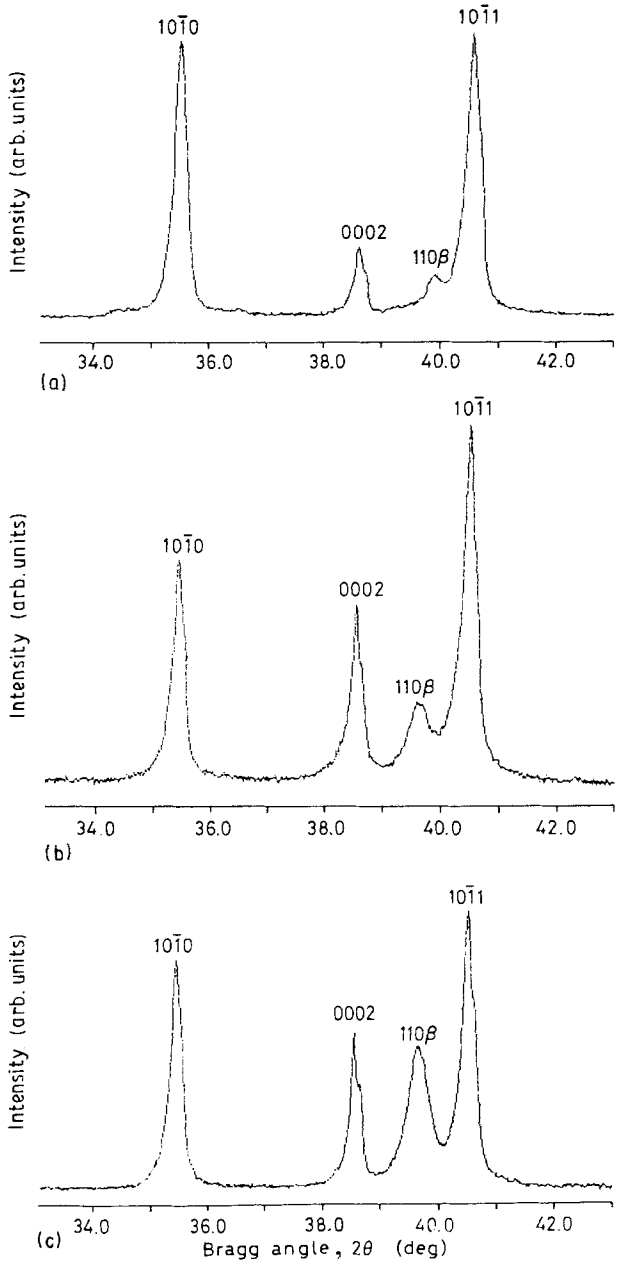

Figure 3 X-ray diffractometer traces showing intensities of $(1\,0\,\bar{1}\,0)$, $(0\,0\,0\,2)$ and $(1\,0\,\bar{1}\,1)$ α-phase reflections and the $(1\,1\,0)$ β-phase reflection: (a) as-received, (b) after superplastic deformation at $4.2 \times 10^{-4} s^{-1}$, (c) after non-superplastic deformation at $1.05 \times 10^{-2} s^{-1}$ (longitudinally stressed test pieces of Ti–6Al–4V).

conditions, with the opposite effect on intensities under non-superplastic conditions (Fig. 3a to c).

3.3. T- and ST-orientation test pieces

After superplastic deformation very similar changes were found in the T and ST orientations to those for the L orientation, namely only a small change in the α-phase texture (Figs 4b and 5b) but a large loss in the β-phase texture intensity (Figs 4e and 5e).

After non-superplastic deformation texture changes were also similar to those found for the L-orientation test pieces, i.e. very little change in the α-phase (Figs 4c and 5c) and the development of a $\langle 1\,1\,0 \rangle$ fibre texture in the β-phase (Figs 4f and 5f).

4. Discussion

The major point to emerge from this investigation is the markedly different sensitivities to the applied strain rate of the α- and β-phases in Ti–6Al–4V, irrespective of testing direction, when this alloy is deformed at 928 °C.

The phase proportions by volume existing at room temperature and at 928 °C are shown schematically in Fig. 6. At room temperature the microstructure consists of ~90% α and ~10% β, whereas at 928 °C ~44% of the α-phase has transformed to β-phase to give an approximately 50:50 mixture [7]. On subsequent cooling to room temperature ~80% of the β-phase (but not necessarily the same β-phase that transformed on heating) transforms back to α-phase to result in, again, an approximately 90:10 mixture. To distinguish between these two forms of α-phase the subscripts p and s [15] will be used to signify primary (non-transforming) and secondary (transforming) α-phase, respectively. It must therefore be borne in mind when analysing textures in Ti–6Al–4V, and in other two-phase titanium alloys at room temperature after deformation at 928 °C, that only ~56% of the α-phase so present will remain as α-phase during

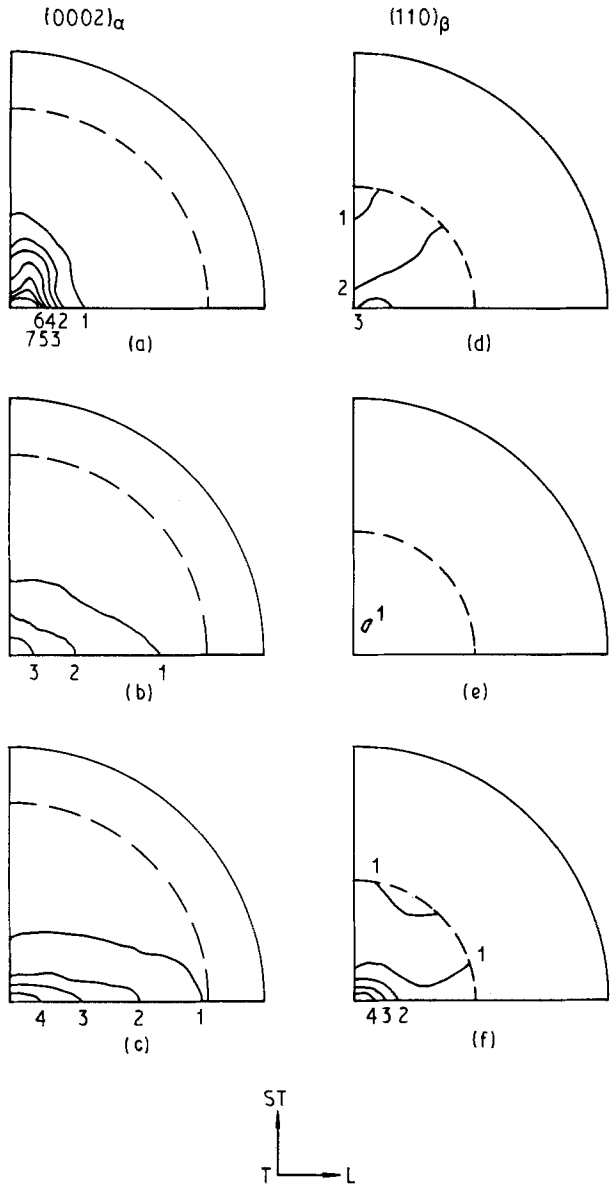

Figure 4 $(0002)_\alpha$ and $(1\,1\,0)_\beta$ pole figures for transversely stressed test pieces of Ti–6Al–4V: (a, d) as-received; (b, e) after superplastic deformation at $4.2 \times 10^{-2} s^{-1}$; (c, f) after non-superplastic deformation at $1.05 \times 10^{-2} s^{-1}$ (contours × random).

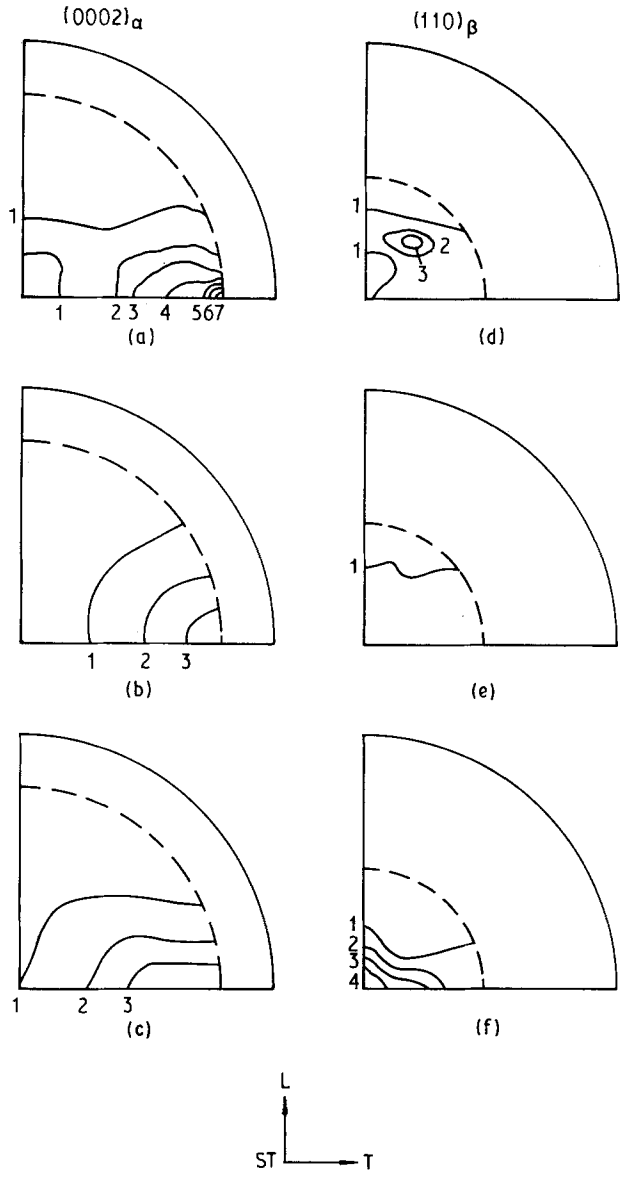

Figure 5 $(0002)_\alpha$ and $(1\,1\,0)_\beta$ pole figures for short-transverse stressed test pieces of Ti–6Al–4V: (a, d) as-received; (b, e) after superplastic deformation at $4.2 \times 10^{-4} s^{-1}$; (c, f) after non-superplastic deformation at $1.05 \times 10^{-2} s^{-1}$ (contours × random).

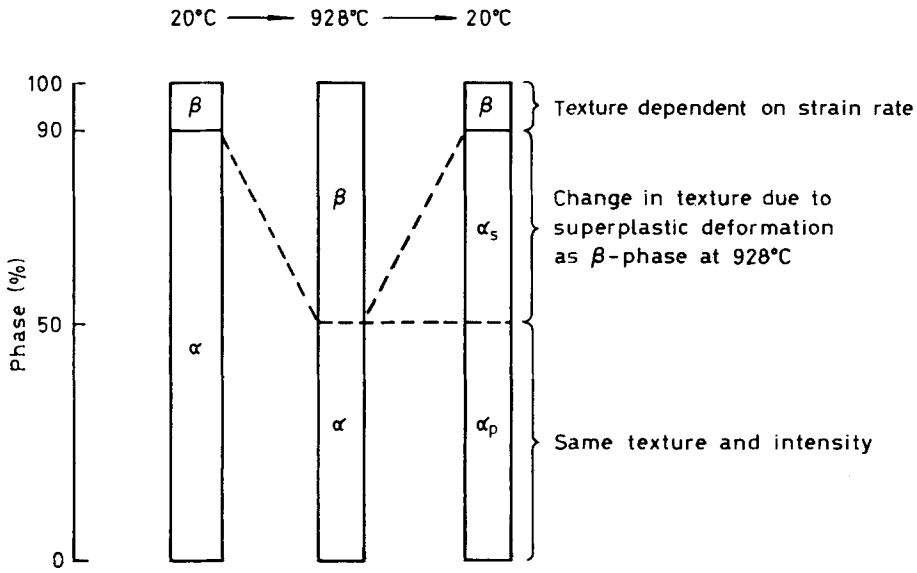

Figure 6 Schematic diagram showing phase transformations and texture changes as a result of a thermal cycle to 928 °C.

the heating and cooling cycle. The other ~44% of the α-phase will reflect the transformation to β-phase, the deformation of the β-phase at elevated temperatures, and then the transformation back to α-phase. Thus to interpret correctly the texture changes in the α-phase it is clearly necessary to consider both forms of the α-phase and the relative properties of the α- and β-phases at 928 °C. From arguments advanced previously [8], the rate-controlling parameter for grain-boundary sliding may be taken as proportional to the product δD_{gb} (where δ is the grain boundary width and D_{gb} the grain boundary diffusion coefficient). Unfortunately there are no values for δ or D_{gb} for titanium alloys, although values of D_v (the volume diffusion coefficient) are in the ratio $D_{v\beta} \approx 100\ D_{v\alpha}$ [16]. Thus if D_v is indicative of the relative values for the $(D_{gb})\alpha$- and $(D_{gb})\beta$-phases, and taking the flow stress (σ) values [17] for the α-phase alloy Ti–SAl–2.5 Sn and the β-phase alloy Ti–15V–3Al–3Sn–3Cr at 900 °C and at strain rates between 10^{-5} and $10^{-2}\ s^{-1}$, which are in the order $\sigma_\beta < \sigma_\alpha$, the data suggest that most, if not all, of the high-temperature deformation will be accommodated in the β-phase – either by grain boundary sliding or plastic deformation. Similar conclusions have been reached previously for (α + β) titanium alloys [17–20]. This situation is not unique, however, since it is similar to that found in α/β brass [21], Cu–P [22] and Pb–Sn [23] alloys, which also consist of a mixture of hard and soft phases. Photoelectron emission microscopy observations of (α + β) titanium alloys [24, 25] offer confirmation of this interpretation, since they show that the β-phase flows around the α-phase during hot deformation. We can then envisage deformation on a model (Fig. 7) modified from that proposed previously [8], where the β-phase (dark) assumes the role of an amorphous medium that flows around the "hard" α-phase (light).

The observations recorded in this paper can now be interpreted as follows. After superplastic deformation the β-phase showed a marked weakening in texture. It is reasonable to conclude, therefore, that the α-phase that formed from it on cooling should also be weakly textured. The α_p, however, should retain its original orientation (except for isolated grains in a cluster that might shear off, (e.g. A in Fig. 7) with the overall effect that essentially all the reported loss in measured α-texture intensity with increasing superplastic strain [5, 7] is due to the progressive removal of the texture in the α_s (which was deformed as β). This is shown schematically in Fig. 8. Such an explanation predicts a maximum texture reduction of ~44%. The observed reduction at a strain of 1.2 is ~40%, which is in good agreement with this prediction. It would be interesting to study larger strains to see if the loss in texture remained unchanged at ~3R. Diffractometer traces suggest that this may well be the case, since a levelling-off in the loss of texture is clearly evident [7].

After non-superplastic deformation the β-phase begins to develop a ⟨1 1 0⟩ fibre texture (often seen in b.c.c. metals [26]). If the Burgers relationship is obeyed [14], then on subsequent transformation to α_s the ⟨0 0 0 1⟩ texture should be enhanced, although this is likely to be complicated by any variant selection. The small increases in intensity at the centre of the (0 0 0 2) pole figures for all three directions (Figs 1c, 4c and 5c) lend some credence to this explanation. Unfortunately, the necking and low elongations obtained under non-superplastic conditions precluded any cross-checking by the post-deformation measurement of Young's modulus, E, which would show any changes in orientation of (0 0 0 2) planes [5, 13]. (Those measured at slow strain rates [5] are not relevant because they are representative of superplastic deformation).

Comments were made earlier on the low residual strains observed in these deformed test pieces of Ti–6Al–4V. Closer inspection of the diffractograms in Fig. 3, however, indicates that peak widths, although narrow, are not the same for both phases. Measured values for the full width at half the maximum intensity (FWHM) of the reflections in Fig. 3 are given in Table II, from which it is clear that line broadening of the (1 1 0) β-phase reflection occurred during superplastic and non-superplastic deformation, whereas no broadening occurred for the α-phase reflections. This line broadening can arise from two sources: strain in

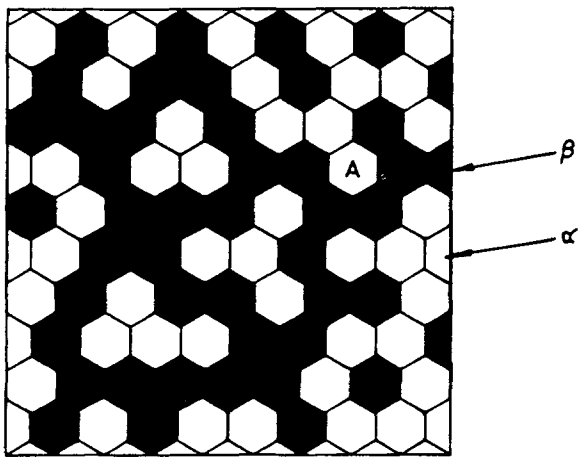

Figure 7 Modified model of the idealized random distribution of α (light) and β (dark) grains in Ti–6Al–4V at 928 °C (after [8]).

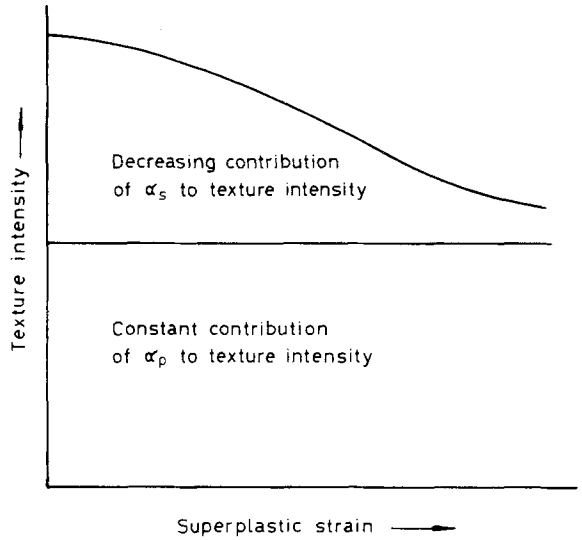

Figure 8 Schematic diagram showing the constant (from α_p) and decreasing (from α_s) contributions to the measured intensity of the α-phase texture.

TABLE II Line-broadening data for α- and β-phase reflections in Ti–6Al–AV alloy as a function of strain rate

Condition	FWHM (deg)			
	$(10\bar{1}0)_\alpha$	$(0002)_\alpha$	$(110)_\beta$	$(10\bar{1}1)_\alpha$
As-received	0.17	0.12	0.25	0.17
Longitudinal $4.2 \times 10^{-4} s^{-1}$	0.15	0.11	0.39	0.14
Longitudinal, $1.05 \times 10^{-2} s^{-1}$	0.16	0.10	0.32	0.15

the lattice, and a small particle size [27]. A contribution due to the size of the β-phase (see Fig. 1 in McDarmaid *et al.* [5]) can be neglected because particle size contributes to line broadening only below ~200 nm [27]. Differences in line widths between the α- and β-phases can therefore be attributed to a greater residual strain in the β-phase lattice. This provides further support for the arguments proposed above, namely that most, if not all, of the high-temperature strain in Ti–6Al–4V is accommodated in the β-phase.

5. Conclusions

Deformation of the Ti–6Al–4V alloy at 928 °C has shown the following.

1. Texture changes subsequently measured at room temperature in the α-phase are relatively insensitive to the applied strain rate in the range $4 \times 10^{-4} s^{-1}$ (superplastic) to $1.05 \times 10^{-2} s^{-1}$ (non-superplastic).
2. Texture changes in the β-phase, under the same conditions, are very sensitive to the applied strain rate, with a marked loss in intensity at superplastic strain rates but with a tendency to change towards a $\langle 1\,1\,0 \rangle$ fibre texture at non-superplastic rates.
3. Superplastic deformation appears to occur almost entirely in the softer β-phase, by grain boundary sliding and plastic deformation.
4. Non-superplastic deformation probably occurs almost entirely in the β-phase, but with a much greater contribution from plastic deformation.
5. The interpretation of high-temperature deformation, by room-temperature analysis, must take into account the effects of the phase transformations that occur between room and elevated temperatures.

References

1. B. P. KASHYAP, A. ARIELI and A. K. MUKHERJEE, *J. Mater. Sci.* **20** (1985) 2661.
2. U. HEUBNER, K. H. MATUCHA and H. SANDIG, *Z. Metallkde* **63** (1972) 607.
3. K. N. MELTON, J. W. EDINGTON, J. S. KALLEND and C. P. BUTLER, *Acta Metall.* **22** (1974) 165.
4. C. P. BUTLER, J. W. EDINGTON, J. S. KALLEND and K. N. MELTON, *ibid.* **22** (1974) 665.
5. D. S. McDARMAID, A. W. BOWEN and P. G. PARTRIDGE, *Mat. Sci. Engng* **64** (1984) 105.
6. *Idem, J. Mater. Sci.* **19** (1984) 2378.
7. *Idem, ibid.* **70** (1985) 1976.
8. P. G. PARTRIDGE, D. S. McDARMAID and A. W. BOWEN, *Acta Metall.* **33** (1985) 571.
9. P. G. PARTRIDGE, A. W. BOWEN, C. D. INGLEBRECHT and D. S. McDARMAID, in "Superplasticity", edited by B. Baudelet and M. Súery (CNRS, Paris, 1985) p. 10-1.
10. A. W. BOWEN, *Adv. X-ray Anal.* **29** (1986) 271.
11. *Idem*, in "Residual Stresses in Science and Technology", Vol. 2, edited by E. Macherauch and V. Hauk, Deutsche Gesellschaft für Metallkunde, Oberursel, 1987) p. 917.
12. R. A. HOLT and J. E. VINEGAR, *J. Appl. Phys.* **48** (1977) 3557.
13. A. W. BOWEN, *Mat. Sci. Engng* **29** (1977) 19.
14. W. G. BURGERS, *Physica* **1** (1934) 561.
15. Data Sheet, *Met. Progr.* **121** (1982) (2) 51.
16. C. DYMENT and C. M. LIBANATI, *J. Mater. Sci.* **3** (1968) 349.
17. S. M. SASTRY, P. S. RAO and K. V. SANKARAN, in "Ti '80", Vol. 2, edited by H. Kimura and O. Izumi (AIME, Warrendale, 1980) p. 873.
18. C. M. HAMILTON, in "Superplasticity", edited by B. Bandelet and M. Súery (CNRS, Paris, 1985) p. 14-1.
19. B. HILDAGO-PRADA and A. K. MUKHERJEE, *Scripta Metall.* **19** (1985) 1235.
20. *Idem*, in Proceedings of 7th International Conference on Strength of Metals, Vol. 2 (Pergamon, Oxford, 1985) p. 835.
21. M. SÚERY and B. BAUDELET, *Res. Mech.* **2** (1987) 163.
22. G. HERRIOT, B. BAUDELET and J. J. JONAS, *Acta Metall.* **24** (1976) 687.
23. A. E. GEKINLI and C. R. BARRETT, *J. Mater. Sci.* **11** (1976) 510.
24. J. MA and C. HAMMOND, in "Titanium Science and Technology", Vol. 2, edited by G. Lütjering (Deutsche Gesellschaft für Metallkunde, Oberursel, 1985) p. 703.
25. C. HAMMOND, A. NICKELLS and N. E. PATON, *Metall* **20** (1987) 199.
26. I. L. DILLAMORE and W. T. ROBERTS, *Met. Rev.* **20** (1965) 271.
27. B. D. CULLITY, "Elements of X-ray Diffraction" (Addison-Wesley, Reading, 1978) p. 284.

Received 31 July
and accepted 29 October 1990